Nonequilibrium Morphology Development in Seeded Emulsion Polymerization. V. The Effect of Crosslinking Agent

Jeffrey M. Stubbs, Donald C. Sundberg

Nanostructured Polymers Research Center, Materials Science Program, University of New Hampshire, Durham, New Hampshire 03824

Received 13 December 2005; accepted 11 January 2006
DOI 10.1002/app.24063
Published online in Wiley InterScience (www.interscience.wiley.com).

ABSTRACT: It is understood that a major controlling factor in the development of latex particle morphology is the extent to which second stage oligomeric radicals can diffuse into the particles after entry from the aqueous phase. This leads to the expectation that any factor which decreases the diffusion rate of second stage radicals should decrease radical penetration, and thus favor the formation of core–shell type morphologies. The occurrence of crosslinking reactions during the second stage may be one such factor, since the branched and crosslinked chains diffuse much more slowly (if at all) than their linear counterparts. This paper addresses the effect of the addition of crosslinking agent (a divinyl monomer) during the second stage polymerization on particle morphology. It is shown experimentally that, contrary to what one might expect, crosslinking during the second stage has very little, if any, effect on morphology. Modeling suggests that the reason is that the probability for radicals to develop a branch before penetrating a significant distance into the particles is very low (under conditions where full penetration is possible in the absence of crosslinking agent), especially for what is considered to be typical concentrations of crosslinking agent. © 2006 Wiley Periodicals, Inc. J Appl Polym Sci 102: 2043–2054, 2006

Key words: latices; core–shell polymers; nanocomposites; emulsion polymerization; morphology

INTRODUCTION

Composite latices, containing two or more phase-separated polymers within each latex particle, have a range of industrial applications, including architectural and paper coatings, adhesives, and impact modifiers (Ref. 1 and references therein). The structure, or morphology (a core–shell being only one possible morphology), within the particles has a large impact on the properties of the products derived from these latices.[2] Thus, understanding how to control particle morphology is of vital importance. These latices are produced by starting with a "seed" latex (or one produced during a first stage) and polymerizing a different monomer (or comonomers) within the previously formed seed particles during a second stage. It is well known that morphology can be controlled by either thermodynamic or kinetic factors, with thermodynamic control, resulting in equilibrium structures, being by far the most well understood.[1,3–5] The equilibrium morphology is the one that minimizes the total interfacial free energy associated with the composite particle. Under kinetic control, morphology development is dependent on the relative rates of polymerization and diffusion within the latex particles during the second stage polymerization. This article is the fifth in a series that reports on morphology development in latex particles under kinetically controlled conditions. The previous four articles[6–9] have shown quite conclusively that the primary control factor is the extent to which second stage oligoradicals, which enter the particles from the aqueous phase, can penetrate into the interior of seed particles by diffusion.

The importance of crosslinking in latex technology is exemplified by a number of industrial products. Examples include impact modifier particles (crosslinking in the core), hollow latex particles used for opacifiers (crosslinking in the shell), stimuli-responsive hydrogels (crosslinking in the shell or both), and latex interpenetrating polymer networks (IPNs) or semi-IPNs (crosslinking in either the shell or the core).

Our interest in particle morphology led us to investigate the effect of crosslinking during the second stage polymerization. We did this by considering how it may affect the penetration of second stage polymer radicals and subsequently control the particle morphology. Once a radical chain becomes incorporated into a crosslinked network it will no longer be able to diffuse. In fact, De Gennes has predicted that as soon

Correspondence to: J. M. Stubbs (jstubbs@cisunix.unh.edu).
Contract grant sponsor: UNH Latex Morphology Industrial Consortium (Arkema, DSM NeoResins, Rohm and Haas).

as a chain develops a branch diffusion by reptation will effectively cease,[10] so radical penetration may only proceed until the radical chain develops a branch. Thus, one might expect crosslinking during the second stage to decrease radical penetration, but this conclusion may not be so straightforward. Calculations show that most penetration occurs within the first 10–20 propagation steps after entry from the water phase.[6,7] Typical levels of crosslinking agent (XLA) are on the order of a few percent or less in the monomer. The probability of a very short radical both incorporating a crosslinker molecule and developing a branch, or reacting with a residual double bond in another previously formed chain, may often be quite low. In such cases XLA is expected to have a negligible effect on penetration.

In addition to radical penetration, polymer phase separation and rearrangement are also very important processes in morphology development under kinetically controlled conditions. Crosslinking would be expected to hinder both processes by producing many more restricting entanglements due to the network structure, as in an IPN or semi-IPN. This in fact may be where the largest effect of crosslinking on particle morphology should be expected.

A number of studies on latex particle morphology report on the use of crosslinking in the seed particle only.[4,5,11–14] Crosslinking in the seed particle has been modeled by Durant and Sundberg[4] using thermodynamics and presented with accompanying experiments to validate the model.[5] The results show that crosslinking in the seed imparts elastic forces that hinder subsequent volumetric expansion of the seed particle and favors the development of core–shell morphologies or other structures where the second stage polymer is located on the surface of the particle.

Many references report on work utilizing crosslinking in both stages, thus producing polymer IPN's. This often prevents phase separation from occurring completely, or only allows it to occur to a limited extent.[15–20] Sionakidis et al.[21] reported on the preparation of latex IPN's using XLA in both stages and noted that the seed is partially penetrated by the second stage polymer, yielding increasing amounts of second stage network copolymer in the shell region of the particles. These findings seem related to our current query into radical penetration. However, given that their seed was both crosslinked and having a T_g much greater than the reaction temperature, it is unclear whether this condition of partial penetration is due to the crosslinking in the second stage or simply by the seed latex properties (T_g and elasticity) which hinder diffusion and favor forming core–shell morphologies.

In the production of hollow particles, crosslinking is used in the second stage only to produce a core–shell particle with a crosslinked shell. Devon and McDonald have recently reviewed this topic.[22] The route towards forming hollow latex particles referred to as the hydrocarbon encapsulation method has the most relevance here. This involves forming a shell of a thermoplastic, crosslinked polymer around a seed particle core composed of a hydrocarbon or a low MW polymer. Shell formation relies on having a thermodynamic driving force (interfacial energies) to form a core–shell morphology. Crosslinking does not necessarily favor the formation of a core–shell structure, but simply provides the shell with mechanical stability so that the morphology can be retained when the hydrocarbon core is later extracted to form a hollow particle. Other papers have reported on latex systems with core–shell structures, using crosslinking in the second stage, in which the mechanism of morphology formation is likely to be similar to that in the production of hollow particles by hydrocarbon encapsulation.[23–25]

There are other studies which consider latex particle morphology development in which crosslinking was utilized to some extent exist.[26–31] However, none of these studies were specifically aimed at investigating whether or not crosslinking during the second stage has an effect on radical penetration and morphology development. It is ironic that the study that perhaps comes the closest to considering the question of the effect of crosslinking on radical penetration is one that does not consider core–shell type particles at all. Matsumoto et al.[32] reported on the emulsion copolymerization of MMA and allyl methacrylate (AMA, a crosslinker). In their system (with AMA) most of the crosslinking developed later in the polymerization and they concluded that the core of the particle was rich in PMMA while the shell contained more crosslinked P(MMA-AMA). They supposed that the penetration of radicals into the particle core was suppressed by the high T_g of the P(MMA/AMA) particle and by the formation of a crosslinked network in the shell. However, they did not make the distinction between which of the two factors was controlling, and since this system is not phase separating there was no morphological evidence to support their interpretation.

The present article specifically investigates, using both modeling and experimentation, the effect of crosslinking during the second stage on particle morphology from the point of view of whether or not this decreases radical penetration. Experiments used a noncrosslinked, polar, methacrylic seed polymer and a nonpolar styrene containing second stage polymer. All polymerizations were conducted under semibatch conditions with varying concentrations of XLA (a divinyl monomer) added to the second stage comonomer feed to achieve varying extents of crosslinking. Particle morphology was characterized mainly using TEM (of microtomed sections) and temperature-modulated differential scanning calorimetry (TM-DSC)

DESIGN OF THE EXPERIMENTAL LATEX SYSTEM

A number of specific characteristics were desired for the experimental latex system to allow the proposed questions to be answered as well as to facilitate the experimental analysis. These characteristics are listed individually. (1) An inverted core–shell equilibrium morphology was desired so that there would be a driving force to form the second stage polymer within the interior of the particle. (2) It was desired to have a completely uncrosslinked seed polymer to avoid the presence of elastic forces that would prevent the expansion of the seed polymer during the second stage polymerization. Thus, acrylic monomers were avoided in favor of methacrylic monomers, as the former can lead to gel formation through a hydrogen abstraction mechanism.[33] (3)The T_g of the seed polymer should be well below reaction temperature so that linear second stage polymer radicals easily penetrate the seed particles. (4) The T_g of the second stage polymer should be below reaction temperature. In conjunction with the low T_g of the seed polymer, this ensures that, in the absence of crosslinking, phase separation should occur quite easily and affords the opportunity to observe whether or not crosslinking during the second stage decreases the ability of the polymers to phase separate. (5) The seed polymer should be entirely methacrylic and the second stage polymer should contain some styrene to facilitate TEM analysis (this makes it possible to selectively stain the second stage polymer). (6) There should be a significant difference between the T_g's of the seed and second stage polymers to allow the degree of phase mixing between the two polymers to be determined via DSC measurements. (7) Both polymers should have T_g's in the vicinity of room temperature or greater to facilitate microtoming TEM samples, which is vital for determining the extent of penetration of the second stage polymer.

To achieve these conditions the seed comonomers chosen were hydroxypropyl methacrylate (HPMA) and hexyl methacrylate (HMA). HPMA is very polar (much more than MMA) and has a high T_g in the dry state (measured to be 125°C). HMA produces a low T_g polymer (measured to be ~ -30°C) but is nonpolar. The specific seed copolymer produced had a composition of 35HPMA/65HMA by weight and a T_g of 40°C. The hydrophilic nature of this copolymer was confirmed by measuring the SDS adsorption area, using a conductometric titration method described elsewhere,[34] as will be discussed later. The second stage copolymer was an 80% styrene and 20% butyl acrylate by weight. This copolymer is stainable with RuO_4 for TEM analysis, is nonpolar, and has a T_g close to 70°C. Ethylene glycol dimethacrylate (EGDMA) was used as the crosslinking agent in the second stage polymerizations, which all had a stage ratio of 100%. All polymerizations (both seed and second stage) employed starve fed conditions to avoid compositional drift and were conducted at 70°C.

MODELING

We have assumed that as soon as a polymeric radical becomes branched it will cease to penetrate into the particle, following the predictions of De Gennes.[10] The question then becomes whether or not branching will occur early enough after the oligomeric radical enters the particle to have a significant effect on penetration.

The quantification of radical penetration into the particle followed the same approach as utilized previously.[6,7] We add to this approach a calculation of the probability that the radical will become branched. Of course, this probability increases with time as the radical grows (as does the extent of penetration). For a rough approximation we note the point in time where the probability for branching becomes equal to unity, and compare the fractional penetration value, FP (the distance diffused divided by the particle radius), at this moment to the FP that the radical would have attained if it never branched at all. This simple approach provides some insight into the question at hand.

A radical can develop a branch either by (1) having another radical react with one of the pendant double bonds in its own chain or (2) itself reacting with a pendant double bond in another chain. Both possibilities arrest the diffusion (penetration) of the radical. Penetration and probability for branching are followed as a function of time, using a stepwise approach with the time step related to the propagation frequency, as this is the natural time step for the penetration calculations.[7] The probability of a separate radical reacting with a pendant double bond in the "penetrating radical" chain per time step is defined as $P_{\mathrm{xA},i}$ and given by:

$$P_{\mathrm{xA},i} = \frac{N_{\mathrm{pend}} k_{p,\mathrm{e2}} [P^{\bullet}_{\mathrm{tot}}]}{k_p[M] + N_{\mathrm{pend}} k_{p,\mathrm{e2}} [P^{\bullet}_{\mathrm{tot}}]} \tag{1}$$

where N_{pend} is the number of pendant double bonds in the chain, $k_{p,\mathrm{e2}}$ is the propagation rate coefficient for a pendant double bond, and $[P^{\bullet}_{\mathrm{tot}}]$ is the total radical concentration in the particle. Since the frequency of propagation reactions is vastly greater than the frequency of transfer reactions, eq. (1) can be approximated by

$$P_{\mathrm{xA},i} = \frac{N_{\mathrm{pend}} k_{p,\mathrm{e2}} [P^{\bullet}_{\mathrm{tot}}]}{k_p[M]} \tag{2}$$

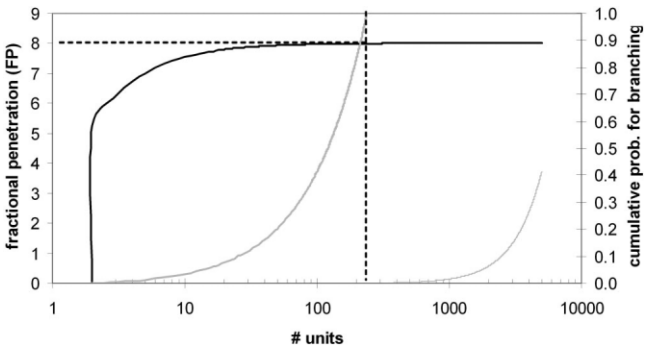

Figure 1 Expected effect of crosslinking on penetration for 1% EGDMA. Thick black line: fractional penetration; thick gray line: total probability for branching; thin gray line: probability for branching by another radical reacting with a pendant double bond in the "penetrating" radical.

Assuming that the divinyl monomer is incorporated into the chain at the same concentration that it is present in the monomer (which should be the case at steady state during a starve fed polymerization for typical reactivity ratios), N_{pend} is directly related to the mole fraction of divinyl monomer in the monomer feed, x_{xla}, and the number of monomer repeat units in the chain, i.

$$N_{\text{pend}} = ix_{\text{xla}} \tag{3}$$

The probability of the penetrating radical reacting with a pendant double bond in another polymer chain is defined as P_{xB} and approximated by

$$P_{\text{xB}} = \frac{k_{p,\text{e2}}[\text{PEND}]}{k_p[M]} \tag{4}$$

where [PEND] is the concentration of pendant double bonds. The total probability of branching per time step, P_i, is given by

$$P_i = P_{\text{xA},i} + P_{\text{xB}} \tag{5}$$

and the cumulative probability of branching is simply

$$P_{\text{cum}} = \sum_{z}^{i} P_i \tag{6}$$

To perform these calculations, one requires values for diffusion coefficients, propagation rate coefficients for the primary (main chain, $k_{p,\text{e1}}$), and secondary (pendant, $k_{p,\text{e2}}$) double bonds of the divinyl monomer, and the various concentrations [M], [$P^{\bullet}_{\text{tot}}$], and [PEND]. The KMORPH software[35,36] was utilized to estimate these concentrations. Further details of this process are provided elsewhere.[37] Diffusion coefficients were estimated using a semiempirical method described previously.[38] For the purposes of this work the values of $k_{p,\text{e1}}$ and $k_{p,\text{e2}}$ for the divinyl monomer, EGDMA, were assumed to be equal to the k_p value for MMA based on knowledge that k_p does not vary significantly through the methacrylate family of monomers.[39] This assumption may lead to some error but should still allow one to obtain a reasonable understanding of radical penetration during crosslinking reactions.

Figure 1 shows the results for the case of using 1 wt % EGDMA in the monomer feed for our chosen experimental conditions. Several features become apparent, first and foremost being that the radical fully penetrates (fractional penetration values in excess of unity) into the particle interior even before the first propagation step. This fact alone makes it unlikely that crosslinking in the second stage will have any effect on the penetration of radicals. This rapid penetration is of course due to the softness of the seed polymer at the reaction temperature. The second point is that the probability of another radical branching to one of the pendant double bonds in the penetrating radical chain, P_{xA}, is insignificant compared to the total probability of branching. Thus, if the radical is going to experience branching before termination, it is far more likely that this will occur by it reacting with a pendant double bond in another chain.

A third important feature of Figure 1 is that the probability of branching does not reach unity until the radical is about 200 units long, and by then all penetration is essentially finished. This shows that crosslinking should not be expected to have any effect on penetration in this experiment with 1% EGDMA.

Given that Figure 1 predicts no effect of crosslinking on penetration at 1% EDGMA, higher concentrations of 10% and 50% were considered. Figure 2 shows the predictions for the 10% case and it is now observed that the probability for branching reaches unity when the radical chain is only 29 units long. However, this is still not quickly enough to have any effect on radical penetration.

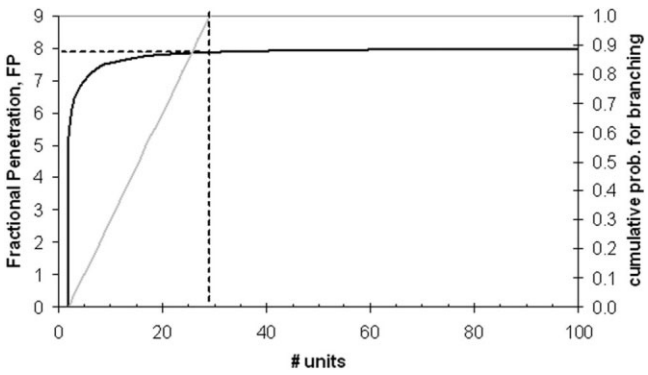

Figure 2 Expected effect of crosslinking on penetration for 10% EGDMA. Black line: fractional penetration; gray line: total probability for branching.

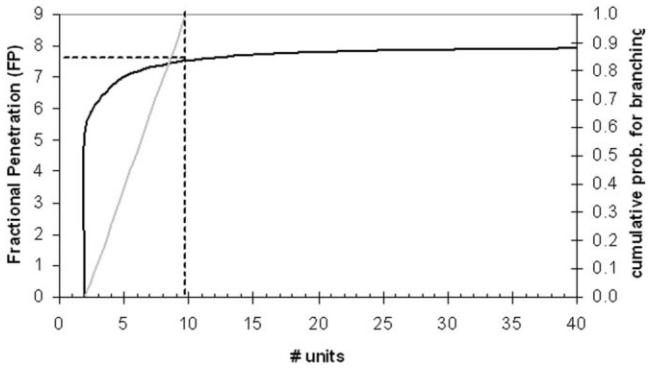

Figure 3 Expected effect of crosslinking on penetration for 50% EGDMA. Black line: fractional penetration; gray line: total probability for branching.

Figure 3 shows the predictions for the 50% case. Here, branching is expected to occur by the time the radical reaches only 10 units, but again, the radical has already fully penetrated the particle by this time. Thus, even in this extreme case of 50% EGDMA by weight, the expected effect on penetration is not very large.

One possible criticism of this conclusion is that we have chosen the system poorly and would not expect an effect on penetration simply because penetration is too rapid in the present system due to its low T_g seed polymer (compared to reaction temperature). However, one must keep in mind that the FP value is directly proportional to the distance diffused. The shape of the FP versus chain length curves remain the same for other systems, including those with higher T_g seed polymers, and are such that the majority of the distance penetrated occurs while the radical is very short. Therefore, in any system, crosslinking will only have an effect on penetration if radicals become branched within the first several propagation steps. The probabilities in Figures 1–3 show that this is very unlikely, even for concentrations as high as 50% EGDMA.

Another possible case that is interesting to consider is one in which the z-mer value is much longer than 2 (the present value for styrene monomer with persulfate initiator[40]). Figure 4 shows an example, for otherwise the same system considered in Figure 3 (50% EGDMA), where the radical does not enter the particle until it is 12 units long. As in Figures 1–3, full penetration is reached before the radical is likely to become branched, so no effect on radical penetration should be expected.

EXPERIMENTAL

Chemicals

Styrene (St), butyl acrylate (BA), hexyl methacrylate (HMA), hydroxypropyl methacrylate (HPMA), and EGDMA monomers (Acros Organics, NJ) were passed through a column of alumina adsorption powder (80–200 mesh, Fisher Scientific) to remove inhibitors and stored at −10°C prior to use. Potassium persulfate, (KPS, analytical grade, Acros Organics) analytical grade sodium bicarbonate (EM Science, NJ), and sodium dodecyl sulfate (99%, Acros Organics) were used as received. Deionized water from a Corning Mega Pure™ D2 water purification system was used in all experiments.

Capillary hydrodynamic fractionation

Particle sizes were measured using capillary hydrodynamic fractionation using a CHDF 2000 from Matec Applied Sciences. The instrument was calibrated over the range from 30 to 700 nm using particle size standards (polystyrene latices) obtained from Seradyn.

Temperature-modulated differential scanning calorimetry

The glass-transition temperature (T_g) of the seed polymer was determined using differential scanning calorimetry using a TA Instruments Q100 DSC. Composite particles were also studied by TM-DSC to determine the extent of phase separation, or amount of phase mixing, between the seed and second stage polymers. Details about this method have been reported previously.[34] All measurements were performed under temperature-modulated conditions with an underlying heating rate of 3°C/min, a modulation amplitude of 3°C and a modulation period of 60 s.

Gel content and crosslink density of crosslinked polymers

The latices were dried in ambient air to obtain dry polymer, which was added to either acetone (for gel

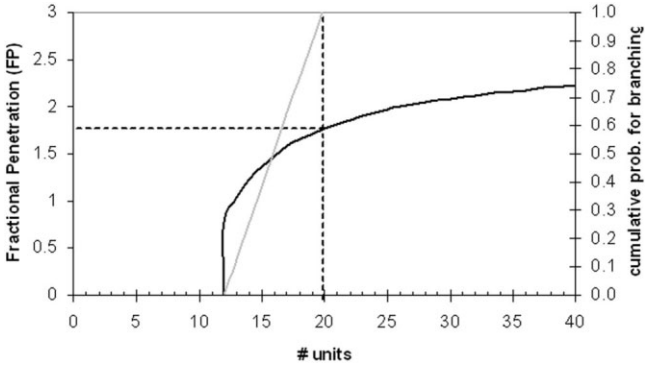

Figure 4 Expected effect of crosslinking on penetration for 50% EGDMA with a larger initial degree of polymerization for the penetrating radical. Black line: fractional penetration; gray line: total probability for branching.

content determination) or THF (for crosslink density determination). In the experiments that did not use crosslinking (the seed polymer and one experiment without crosslinking) the samples dissolved completely to yield a clear, transparent solution. For the crosslinked samples, the solutions were observed to be cloudy, indicating that the crosslinked second stage polymer was present as separated microgel particles which were expected to be on the order of the latex particle size or less (before swelling).

To determine the gel fraction, the dispersed microgel particles were separated from the acetone solutions (0.5 wt % total polymer) by centrifugation [3300 RPM (1580G) Clay Adams Dynac Centrifuge]. Acetone was preferred as the solvent over THF for centrifugation because it has a significantly lower density and lower viscosity, and both factors increase the settling velocity of the microgel particles. These solutions separated effectively upon centrifugation within several hours, and allowed the gel fraction (the sediment) to be easily separated, dried and weighed. The gel fraction was calculated as the mass of the dry microgel polymer recovered divided by the total mass of polymer in the centrifuge tube.

The crosslink density of polymers was determined by an equilibrium swelling method and is related to the extent to which the polymer swells in a good solvent according to:[41]

$$\ln(1-\phi_p)+\phi_p+\chi\phi_2^2=\frac{\rho_p V_1}{M_c}\left(1-\frac{2M_c}{M}\right)\left(\frac{\phi_2}{2}-\phi_2^{1/3}\right) \quad (7)$$

where ϕ_p is the volume fraction of polymer in the swollen gel, ρ_p is the polymer density, V_1 the molar volume of the solvent, χ is the polymer-solvent interaction parameter, M is the molecular weight of the primary chain, and M_c is the average molecular weight of the polymer chain segments in between crosslinks. M_c serves as a measure of the crosslink density (crosslink density is simply equal to $1/M_c$).

The difficulty involved in the experimental measurements was in obtaining the crosslinked polymer in a form where it could be swollen as a cohesive piece, so that the swollen gel could be removed from the solvent and weighed in the swollen state. This was not possible with the cloudy dispersions discussed above. To overcome this, cloudy dispersions were prepared at 5% polymer in THF, and then dried in the dark at 30°C under a nitrogen atmosphere to obtain a film. These films could be cut into manageable sections and swollen in solvent, and the swollen film would remain cohesive and could be removed from the solution and weighed in one piece. The volume fraction of polymer in the swollen film, ϕ_p, was calculated from the swollen and unswollen masses of the films, and then used to calculate M_c from eq. (1). For each sample, measurements were made on four separate sections of film to obtain an average value and assess reproducibility.

Transmission electron microscopy

A small amount of the composite latex was mixed with a film-forming latex, (called the host latex) and a small amount of the mixture was dried in a BEEM® capsule. The host latex polymer was a copolymer of hexyl methacrylate (HMA) and hydroxy propyl methacrylate (HPMA) (65HMA:35HPMA by weight) with a dry T_g of 40°C. The composite latex was mixed with the host to provide a volume ratio of ~15% composite particles. The remaining space in the BEEM capsule was filled with epoxy to allow the sample to be grasped by the calipers of an ultramicrotome. Thin sections (~60 nm) were sectioned using a diamond knife and collected on uncoated copper TEM grids (3 mm diameter, 300 or 400 mesh). The sections are later stained in ruthenium oxide (RuO_4) vapor for 5–10 min. Polymer that contains residual double bonds, including that with incorporated styrene monomer, is selectively stained while that without double bonds is not. The stained polymer then appears darker in the TEM. The sections were then viewed in either a JEOL 100S TEM at a power of 80 keV, or a Leo 922 TEM at a power of 120 keV. It is noted that the host polymer is the same copolymer as the seed copolymer in this case. This brings up the question about whether or not diffusion of polymer chains across interparticle boundaries occurs to an extent which alters the morphology of the composite particles being studied. However, in many of the TEM images ([Fig. 10(A)] for instance), the boundaries between the embedding latex particles remain visible, indicating that relatively little interparticle chain diffusion has occurred.

Seed latex preparation

The seed latex was grown from a polystyrene pre-seed latex having a particle diameter of only 30 nm to allow precise control over the final particle size. This pre-seed was prepared in our laboratory using an emulsion polymerization process employing an unusually high level of surfactant (SDS), the details of which are beyond the scope of this paper. The solid content of the pre-seed latex was 3.6% and the surfactant and residual initiator and buffer had been previously removed with ion exchange resins. Given that the targeted final diameter of the seed latex particles was 180 nm and this required a seed : pre-seed volume ratio in excess of 200, the presence of this tiny amount of polystyrene in the p(HMA-HPMA) seed particles can be neglected. To achieve starve fed conditions throughout the seed particle growth reaction, the monomer feed process was divided into three periods.

TABLE I
Recipe for the Growth of the P(HMA-*co*-HPMA) Seed Latex

Pre-seed latex (g)	38.6
Water (g)	602.8
KPS (g)	0.50
$NaHCO_3$ (g)	0.50
SDS (initial) (g)	0.36
SDS charge 1 (g)	0.71 g in 19.6 g water at ~5 h
SDS charge 2 (g)	0.48 g in 10.7 g water at ~7 h
SDS charge 3 (g)	0.32 g in 9.3 g water at ~9 h
Total monomer (g)	302.5
Monomer feed period 1	
Feed rate and time	10 g/h for ~2 h
Total feed (g)	20.1
Monomer feed period 2	
Feed rate and time	20 g/h for ~3 h
Total feed (g)	60.0
Monomer feed period 3	
Feed rate and time	54.7 g/h for ~4 h
Total feed (g)	222.4

In the first period the monomer was fed very slowly and was incrementally increased in the second and third periods of the reaction. This strategy prevented significant compositional drift and produced a copolymer with a single T_g in the desired range of 40°C. This latex was used as the seed in all subsequent second stage polymerizations. The experimental recipe and conditions employed to produce this seed are provided in Table I.

Second stage polymerizations

The appropriate amounts of seed latex (from Table I), water, SDS, and $NaHCO_3$ were added to a reactor under nitrogen and the temperature was increased to the reaction temperature of 80°C. No additional KPS was added initially as there was enough remaining in the seed latex, but additional KPS was added in increments during the polymerization to maintain a relatively constant rate of radical production. The ratio of styrene to butyl acrylate was 80/20 by weight, and this mixture was fed to the reactor over a period of 2 h. The total amount of monomer was calculated to provide a stage ratio of 100%. Crosslinking experiments were carried out with the EGDMA added directly to the monomer stream at several low concentrations (0%, 0.1%, 0.25%, 0.5%, and 1.0% by weight of monomer) which are typical of emulsion polymerization, as well as at two very high concentrations (10% and 50%). The basic recipe for the second stage polymerizations is shown in Table II.

RESULTS AND DISCUSSION

Characterization of the seed latex

The number average (D_n) and weight average (D_w) particle sizes reported by the CHDF analysis were 175 and 193 nm, respectively, (polydispersity, D_w/D_n = 1.1). Surfactant titrations, performed according to the methods described elsewhere,[34] were used to confirm the polar nature of the copolymer by comparing the measured adsorption area of SDS on the seed polymer surface to other known values for polymers of known polarity. Several titrations were performed and the average adsorption area was determined to be 369.5 ± 4.2 Å^2/molecule. This is significantly higher than the value we have measured for poly(methyl acrylate) (PMA, 160 Å^2/molecule) and confirms that the polymer is indeed very polar. DSC was used to verify that the T_g of the seed polymer was in the desired range, and that only one single glass transition was present. The T_g was measured to be 40°C.

TABLE II
Basic Recipe for the Second Stage Polymerizations

Seed latex (g)	63.6
Water (g)	116.4
SDS (g)	0.16
$NaHCO_3$ (g)	0.05
KPS (initial) (g)	0 (enough remaining in seed latex)
KPS additions	
(0.01*M* solution)	0.75 mL every 30 min for first 2 h
Monomer feed rate (g/h)	9.95
Total monomer feed (g)	19.9
Styrene:BA ratio (wt:wt)	80:20
EGDMA	
(% in monomer)	Variable: 0; 0.1; 0.25; 0.5; 1.0; 10; 50

Results of second stage polymerizations

Kinetics and particle growth

Table III lists the final particle size attained, solid contents, and conversion of second stage monomer. In all cases the final conversion levels are close to 100%. In addition, gravimetric analysis confirmed that all polymerizations proceeded under starve fed conditions (the rate of polymerization was equal to the rate of monomer addition) and the instantaneous conversion remained high throughout the polymerization.

TABLE III
Final Particle Sizes and Conversion Levels for All Second Stage Polymerizations

% EGDMA	Solid content (%)	Conversion of second stage monomer (%)	D_w (nm)	D_n (nm)
0	20.08	101.0	223.8	120.0
0.1	19.83	99.3	225.8	128.6
0.25	20.60	103.7	226.4	128.6
0.5	19.48	93.0	224.7	129.7
1.0	19.83	99.3	225.5	128.1
10	20.31	100.6	227.6	161.0
50	20.12	99.1	237.8	207.0

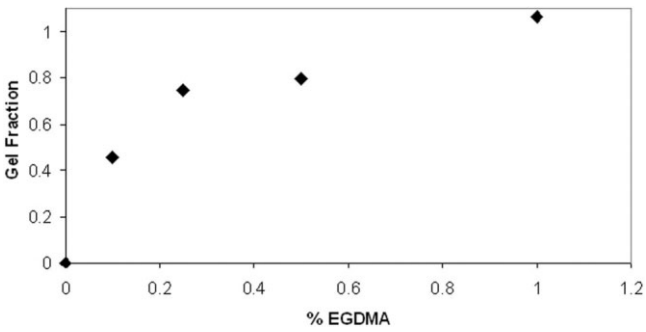

Figure 5 Gel fraction of the second stage polymers.

The particle size analysis shows unexpectedly large differences between the weight and number average diameters due to a small population of particles below 100 nm that were significantly smaller than the average size. This may suggest that some amount of secondary nucleation did occur during the second stage polymerization. However, in all cases the small particle population corresponds to only about 5% by weight of the total particles, and it is clear that most of the second stage polymer was polymerized within the pre-existing seed particles as evidenced by the fact that the weight average diameter (D_w) increased from 193 nm for the seed particles to about 225 nm for the composite particles.

Second stage polymer chain characteristics

The gel fractions (% by weight incorporated into the crosslinked network) of the second stage polymers are shown in Figure 5. The polymer with 0% EGDMA dissolved completely in solution, and so there was no gel material to be separated by centrifugation, and this is the reason for the observed 0% gel for this experiment. For the remaining experiments, the gel fraction quickly increased as the concentration of EGDMA was increased, reaching 100% gel when the concentration of EGDMA was only 1%. Given that 1% EGDMA already produced 100% gel, measurements were not performed on the samples with 10 and 50% EGDMA. We assumed that those polymers also have a negligible fraction of linear chains.

The crosslink density was determined by swelling the samples in THF as described previously. The extent of swelling ranged from about 75 times for the sample with 0.1% EGDMA to about 12 times for the sample with 50% EGDMA. When using eq. (1), the molecular weight, M, of the primary chain was assumed to be equal to the number–average molecular weight of the linear second stage polymer chains for the experiment with 0% EGDMA, which was measured by GPC to be 170,000 g/mol. The value of the interaction parameter, χ, was set equal to 0.5 in the calculations due to the high swelling ratios and the fact that χ approaches 0.5 at high solvent concentrations.[39]

Figure 6 shows the calculated crosslink densities. The samples with concentrations up to 1%EGDMA are calculated to have similar degrees of crosslinking, all ranging between 630 and 720 monomer units between crosslinks. The values suggest that a significant fraction of the EGDMA units lead to a crosslink (based on comparison to the mole fraction of the EGDMA in the monomer mixture). For the samples with higher concentrations of EGDMA, 10% and 50%, the M_c/M values are very large compared to what might be expected based on the mole fraction of EGDMA in the monomer mixture. For the sample with 50% EGDMA, a calculated value of M_c/M is still about 200. This value seems particularly unrealistic, as it is expected to be in the range of a few to tens of monomer units for such a high concentration of EGDMA.

We believe that the apparent error in the measured crosslink densities for the 10% and 50% EGDMA experiments are due to experimental difficulties related to keeping the polymer in one coherent piece during swelling measurements. As explained in the experimental section, when polymer recovered by drying the latex was placed in solvent (THF or acetone), cloudy dispersions were obtained. We believe that this shows that the second stage polymer is present as microgel particles which separate from one another when the composite particles are placed in solvent. This situation may be created simply by the particulate nature of the latex, but is more likely due to the phase-separated structure within the particle. As will be shown later by TEM analysis, multiple domains of second stage polymer are formed within each latex particle. Each domain may represent a separate, disconnected microgel domain. It is likely that when the polymer is placed in solvent, the uncrosslinked seed polymer dissolves uniformly, leaving the separate microgel domains (each coming from a separate domain within a latex particle) dispersed in the solvent and producing the cloudy appearance. Our solution to this problem, detailed in the experimental section, is likely

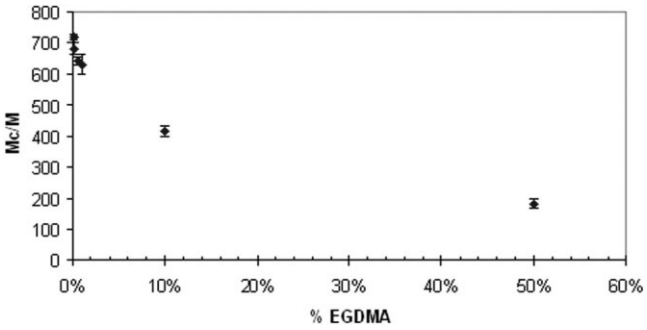

Figure 6 Repeat units between crosslinks in the second stage polymers.

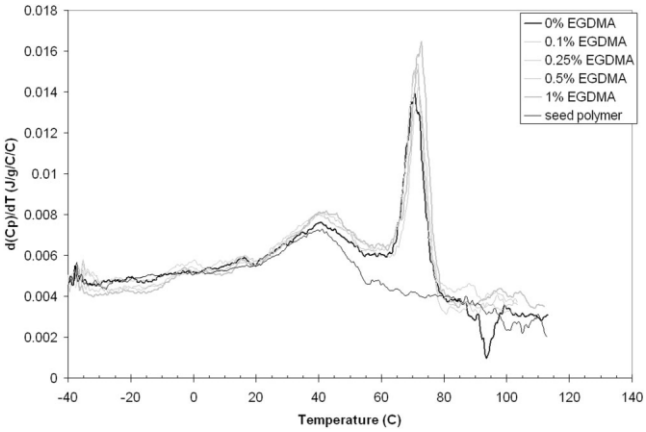

Figure 7 Comparison of DSC traces for all experiments between 0% and 1% EGDMA. The lines corresponding to intermediate concentrations of EGDMA (thin, gray) are not distinguished from one another because they are essentially all the same.

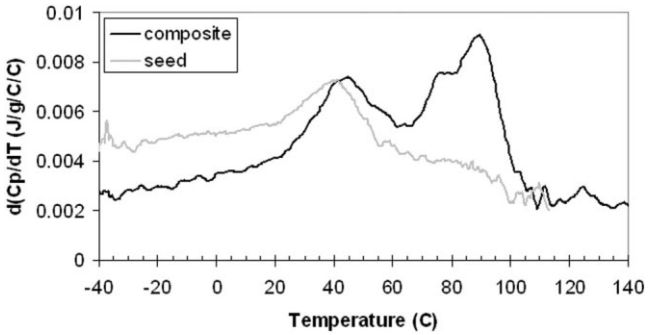

Figure 8 DSC data for the experiment with 10% EGDMA.

to have changed our initial sample such that the resulting crosslink measurements were not meaningful. This also brings into question the crosslink density measurements presented in Figure 6 for the concentrations of EGDMA of 1% and lower. We have not yet addressed this further.

Morphology characterization

DSC analysis

Figure 7 compares the DSC data for the first scans for all experiments with EGDMA concentrations between 0% and 1%. In all cases two distinct peaks are observed with the first, at 40°C, corresponding to the seed polymer and the second, at 70°C, corresponding to the second stage polymer. The presence of two distinct glass transitions suggests that the polymers are well phase separated within the particles. Fitting of the DSC traces using a method described elsewhere[42] (not shown here for the sake of brevity) for the experiments at 0% and 1% EGDMA confirmed the well phase-separated nature of the composite particles. The fitting analysis further indicated that about 35% of the polymer within the particles is present in interfacial regions (having compositions ranging between pure seed and pure second stage polymer). This amount of interfacial material is in line with the occluded morphologies observed by TEM analysis (results discussed in the next section). Thus, the inclusion of EGDMA up to 1% has not changed the ability of the chains to phase separate from one another, even though the second stage polymer is 100% gel at 1% EGDMA.

Figure 8 shows the DSC results for the experiment with 10% EGDMA. The T_g for the second stage polymer is now observed at 90°C instead of 70°C. This increase in T_g may be because the EGDMA concentration is now large enough to have a significant effect on the T_g of the copolymer. Once again, two T_g's are observed. Fitting the data of Figure 9 confirmed that the polymers are largely phase separated, as those at lower concentrations of EGDMA, but that there was slightly more interfacial material (45% of the total polymer). This suggests that at 10% EGDMA the crosslinking of the second stage polymer is starting to have an effect on the ability of the polymers to phase separate, but has not yet prevented phase separation.

The DSC results for the experiment with 50% EGDMA are shown in Figure 9. A very broad transition is now observed ranging from about 0°C all the way to 120°C. This shows that the crosslinking of the second stage polymer has completely prevented phase separation from occurring, and we have now likely produced a semi-IPN.

TEM analysis

The TEM results for the final latex samples for experiments with EGDMA concentrations ranging from 0% to 1% are provided in Figure 10. It is immediately clear that all of the morphologies are completely occluded. Fairly large domains of the dark second stage polymer are located uniformly throughout the particles rather than preferentially towards the outside regions of the

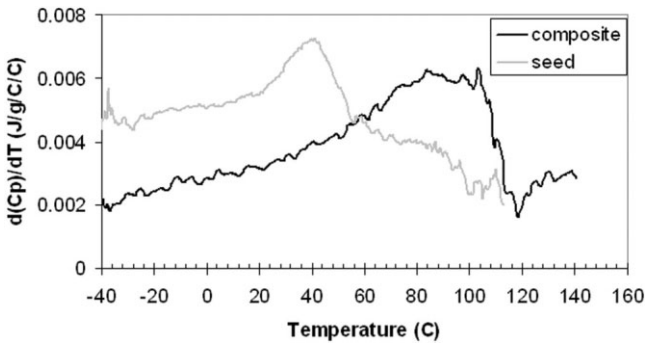

Figure 9 DSC data for the experiment with 50% EGDMA.

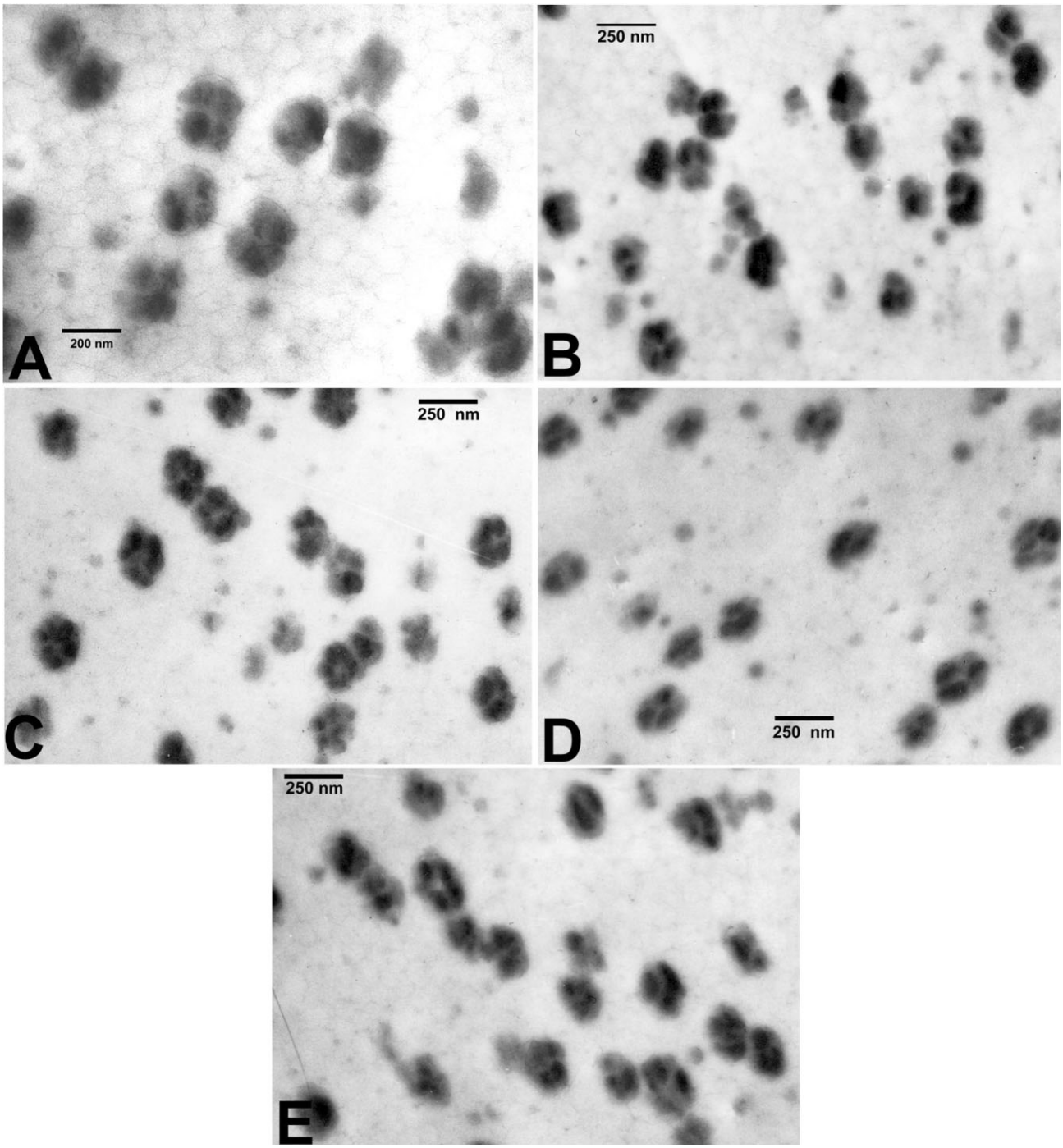

Figure 10 TEM photos of microtomed sections for crosslinking experiments with low EGDMA concentrations. (A) 0% EGDMA; (B) 0.1% EGDMA; (C) 0.25% EGDMA; (D) 0.5% EGDMA; (E) 1.0% EGDMA.

particles. This is in agreement with the predictions that full penetration should be possible and that it should not be impacted by crosslinking at these low EGDMA concentrations. Furthermore, the fairly large domain sizes suggest that these particles are very well phase separated, a result that supports the DSC analysis of the previous section. It is clear that crosslinking during the second stage, at concentrations of EGDMA below 1%, has not had a noticeable effect on morphology development.

The TEM photo for the experiment with 10% EGDMA is shown in Figure 11. An occluded structure is again observed with the domains located uniformly throughout the particle, in agreement with the predictions that full radical penetration should be possible even with 10% EGDMA in the second stage. The average domain size in the particles appears to be smaller and more uniform than the domains observed in the particles produced with lower EGDMA concentrations. This is consistent with the DSC results, which

showed more interfacial material in this experiment compared to lower EGDMA concentrations. Comparison to the earlier experiments may suggest that with lower concentrations of EGDMA, some rearrangement, leading to consolidation of domains, remains possible at EGDMA concentrations of 1% and below but becomes restricted when 10%EGDMA is employed.

The TEM photo for the experiment with 50% EGDMA is shown in Figure 12. The particles now appear very different from those observed at lower concentrations of EGDMA. There is no observable structure within the particles which suggests that the polymers have not phase separated from one another and this is in full agreement with the DSC results of the previous section. It is clear that crosslinking with this high concentration of EGDMA has completely prevented phase separation. It also true that radical penetration was not prevented, because there is no observable region of pure seed polymer in the center of the particles and no T_g for pure seed polymer was observed by DSC. This is once again in agreement with predictions which suggested that crosslinking during the second stage, even at very high levels, should not affect radical penetration but may have an effect on polymer phase separation. We consider this to be an important distinction.

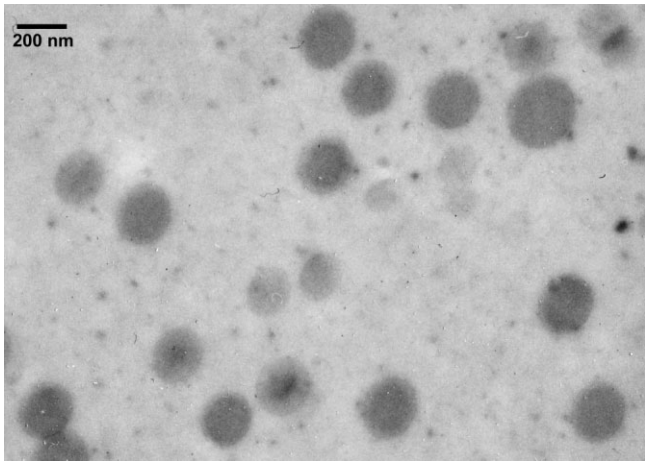

Figure 12 TEM photos of a microtomed section for the experiment with 50% EGDMA.

CONCLUSIONS

It has been shown that crosslinking in the second stage polymerization does not limit the ability of the oligomeric radicals to penetrate into the interior of the seed particles, which is in full agreement with theoretical predictions. Modeling shows that by the time the average radical reacts to form a branched chain it might already have fully penetrated the particle (for systems in which penetration is not already restricted by slow diffusional conditions). This includes systems with considerably high concentrations of divinyl monomer. In cases where radical penetration is already restricted, inclusion of crosslinking agent will not cause a noticeable further decrease in the extent of penetration.

On the other hand, crosslinking in the second stage can hinder the ability of the second stage polymer to phase separate from the seed polymer and also prevent the rearrangement of phase separated domains. This effect is not likely to be evident at low crosslinking agent concentrations (a few percent or less), but intermediate concentrations will lead to smaller phase separated domain sizes and high concentrations can prevent phase separation entirely. Overall, it is shown that low concentrations of crosslinking in the second stage polymerization, in the range of a few percent divinyl monomer, do not result in a noticeable change in the final particle morphology.

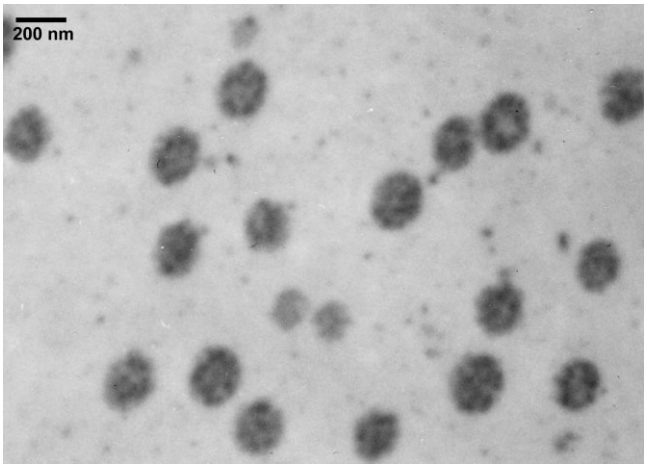

Figure 11 TEM photos of a microtomed section for the experiment with 10% EGDMA.

References

1. Durant, Y. G.; Sundberg, D. C. Polym React Eng 2003, 11, 379.
2. Schuler, B.; Baumstark, R.; Kirsch, S.; Pfau, A.; Sandor, M.; Zosel, A. Prog Org Coat 2000, 40, 139.
3. Sundberg, D. C.; Cassassa, A. J.; Pantazopoulos, J.; Muscato, M. R.; Kronberg, B.; Berg, J. J Appl Polym Sci 1990, 41, 1425.
4. Durant, Y. G.; Sundberg, D. C. Macromolecules 1996, 29, 8466.
5. Durant, Y. G.; Sundberg, E. J.; Sundberg, D. C. Macromolecules 1997, 30, 1028.
6. Stubbs, J. M.; Karlsson, O. J.; Jönsson, J.-E.; Sundberg, E. J.; Durant, Y. G.; Sundberg, D. C. Colloids Surf A 1999, 153, 255.
7. Karlsson, L. E.; Karlsson, O. J.; Sundberg, D. C. J Appl Polym Sci 2003, 90, 905.
8. Stubbs, J. M.; Sundberg, D. C. J Appl Polym Sci 2004, 91, 1536.
9. Stubbs, J. M.; Sundberg, D. C. J Appl Polym Sci 2006, 102, 945.
10. De Gennes, P.-B. Scaling Concepts in Polymer Physics; Cornell University Press: Ithaca, 1979.
11. Segall, I.; Dimonie, V. L.; El-Aasser, M. S.; Soskey, P. R.; Mylonakis, S. G. J Appl Polym Sci 1995, 58, 401.

12. Sommer, F.; Duc, T. M.; Pirri, R.; Meunier, G.; Quet, C. Langmuir 1995, 11, 440.
13. Merkel, M. P.; Dimonie, V. L.; El-Aasser, M. S.; Vanderhoff, J. W. J Polym Sci Part A: Polym Chem 1987, 25, 1219.
14. Dos Santos, F. D.; Fabre, P.; Drujon, X.; Meunier, G.; Leibler, L. J Polym Sci Part B: Polym Phys 2000, 38, 2989.
15. Sperling, L. H. Interpenetrating Polymer Networks and Related Materials; Plenum: New York, 1981; p 2.
16. Meseguer Duenas, J. M.; Gomez Ribelles, J. L. J Therm Anal Calorimetry 2003, 72, 695.
17. Song, M.; Hourston, D. J.; Pollock, H. M.; Shafer, F. U.; Hammiche, A. Thermochim Acta 1997, 304, 335.
18. Hourston, D. J.; Song, M.; Schafer, F. U.; Pollock, H. M.; Hammiche, A. Thermochim Acta 1998, 324, 109.
19. Song, M.; Hourston, D. J.; Shafer, F. U.; Pollock, H. M.; Hammiche, A. Thermochim Acta 1998, 315, 25.
20. Lee, J. S.; Shin, J. H.; Kim, B. K.; Kang, Y. S. Colloid Polym Sci 2001, 279, 959.
21. Sionakidis, J.; Sperling, L. H.; Thomas, D. A. J Appl Polym Sci 1979, 24, 1179.
22. Devon, M. J.; McDonald, C. J. Adv Colloid Interface Sci 2002, 99, 181.
23. Schellenberg, C.; Akari, S.; Regenbrecht, M.; Tauer, K.; Petrat, F. M.; Antonietti, M. Langmuir 1999, 15, 1283.
24. Schellenberg, C.; Tauer, K.; Antonietti, M. Macromol Symp 2000, 151, 465.
25. Kalinina, O.; Kumacheva, E. Macromolecules 2001, 34, 6380.
26. Lu, C.; Pelton, R. Colloids Surf A 2002, 201, 161.
27. Santos, A. M.; Elaissari, A.; Martinho, J. M. G.; Pichot, C. Polymer 2005, 46, 1181.
28. Fujii, S.; Randall, D. P.; Armes, S. P. Langmuir 2004, 20, 11329.
29. Kirsch, S.; Pfau, A.; Stubbs, J.; Sundberg, D. Colloids Surf A 2001, 183, 725.
30. Kirsch, S.; Stubbs, J.; Leuninger, J.; Pfau, A.; Sundberg, D. J Appl Polym Sci 2004, 91, 2610.
31. Dullens, R. P. A.; Claesson, M.; Derks, D.; Van Blaaderen, A.; Kegel, W. K. Langmiur 2003, 19, 5963.
32. Matsumoto, A.; Kodama, K.; Aota, J.; Capek, I. Eur Polym J 1999, 35, 1509.
33. Odian, G. Principles of Polymerization, 4th ed.; Wiley: Hoboken, 2004; p 253.
34. Stubbs, J. M.; Durant, Y. G.; Sundberg, D. C. Langmuir 1999, 15, 3250.
35. Karlsson, O. J.; Stubbs, J. M.; Carrier, R. H.; Sundberg, D. C. Polym React Eng 2003, 11, 589.
36. Stubbs, J. M.; Karlsson, O. J.; Carrier, R. H.; Sundberg, D. C. Prog Colloid Polym Sci 2003, 124, 131.
37. Stubbs, J. M. Ph.D. Thesis, University of New Hampshire, May 2005.
38. Karlsson, O. J.; Stubbs, J. M.; Kalsson, L. E.; Sundberg, D. C. Polymer 2001, 42, 4915.
39. Brandrup, J.; Immergut, E. H.; Grulke, E. A., Eds. Polymer Handbook, 4th ed.; Wiley: New York, 1999.
40. Gilbert, R. G. Emulsion Polymerization: A Mechanistic Approach; Academic Press: London, 1995.
41. Labana, S. S., Ed. Chemistry and Properties of Crosslinked Polymers; Academic Press: New York, 1977; p 261.
42. Stubbs, J. M.; Sundberg, D. C. J Polym Sci Part B: Polym Phys 2005, 43, 2790.